

Performance analysis of Savonius Rotor for Wave Energy Conversion using CFD

Mohammed Aisd Zullah¹⁾, Young-Do Choi²⁾, Kyuhan Kim³⁾, Young-Ho Lee⁴⁾

Abstract : A general purpose viscous flow solver Ansys CFX is used to study a Savonius type wave energy converter in a 3D numerical viscous wave tank. This paper presents the results of a computational fluid dynamics (CFD) analysis of the effect of blade configuration on the performance of 3 bladed Savonius rotors for wave energy extraction. A piston-type wave generator was incorporated in the computational domain to generate the desired incident waves. A complete OWC system with a 3-bladed Savonius rotor was modeled in a three dimensional numerical wave tank and the hydrodynamic conversion efficiency was estimated. The flow over the rotors is assumed to be two-dimensional (2D), viscous, turbulent and unsteady. The CFX code is used with a solver of the coupled conservation equations of mass, momentum and energy, with an implicit time scheme and with the adoption of the hexahedral mesh and the moving mesh techniques in areas of moving surfaces. Turbulence is modeled with the k-e model. Simulations were carried out simultaneously for the rotor angle and the helical twist. The results indicate that the developed models are suitable to analyze the water flows both in the chamber and in the turbine. For the turbine, the numerical results of torque were compared for all the cases.

Key words : Savonius rotor, wave energy, numerical wave tank, efficiency

Nomenclature

Y_{dis} : Wave maker plate displacement
 α : wave amplitude, m
 ω : wave frequency, Hz
 P_{Tave} : average torque power, W
 P_{Wave} : wave power, W
 g : gravitational acceleration, $9.81 \text{ m}^2/\text{s}$
 ρ : water density, 998 kg/m^3
 H_j : Incoming wave height, m
 λ : wave length, m
 T : wave time period, s
 b : width of the chamber opening, m
 d : water depth, m
 τ the average torque
 N : Rotational speed of the turbine, RPM

Most importantly, waves are a regular source of power with an intensity that can be accurately predicted several days before their arrival. Furthermore, wave energy is more predictable than wind or solar energy [1].

There is approximately 8,000 - 80,000 TWh/yr or 1 - 10 TW of wave energy in the entire ocean, and on average, each wave crest transmits 10 - 50 kW per meter [2]. The energy levels depicted in Fig.1 are important to keep in mind when designing any sort of wave power take-off device, but it should also be noted that wave power decreases closer to the shore because of frictional losses with the coast line.

Water waves have energy associated with

1. Introduction

Ocean waves arise from the transfer of energy from the sun to wind then water. Solar energy creates wind which then blows over the ocean, converting wind energy to wave energy. Once converted, this wave energy can travel thousands of miles with little energy loss.

-
- 1) Graduate school, Korea Maritime University
E-mail : zullah@pivlab.net
Tel : (51)410-4940 Fax : (82)51-403-0881
 - 2) Dept of Mechanical Engineering, Mokpo Nat. Univ.
E-mail : ydchoi@mokpo.ac.kr
Tel : (82)61-450-2419 Fax : (82)61-452-6376
 - 3) Kyuhan Kim, Kwandong University
 - 4) Div. of Mech. & Info. Eng., Korea Maritime Univ.
E-mail : lyh@hhu.ac.kr
Tel : (51)410-4293 Fax : (82)51-403-0381

them: kinetic energy of the moving particles and potential energy due to the vertical position of the water from the mean level. The total energy is proportional to the square of the wave height and is equally divided between kinetic and potential energies [3,4]. A higher wave will have more potential and kinetic energies [5]. A number of devices are now developed to extract energy from the waves [3,5,6]. Wave energy is attracting a lot of attention now, as it is available 90% of the time at a given site compared to solar and wind energies which are available 20-30% of the time [7]. According to McCormick [8], there are some basic concepts on which wave energy extraction devices are based. Heaving and pitching bodies make use of the surface displacement of water as an energy source. Pressure devices utilize the hydrostatic and dynamic pressure changes beneath the water waves. Surging wave energy converters capture wave energy as waves enter the surf zone. Cavity resonators make use of the displacement of water in a water column. Particle motion converters obtain energy from the moving water particles. The moving elements of the energy extraction device should have their motions matching those of the orbiting water particles. One of these is a Savonius Type Turbine for wave energy converter which is not well known.

2. Savonius Rotor

Savonius rotor is a unique fluid-mechanical device that has been studied by numerous investigators since 1920s. Applications for the Savonius rotor have included pumping water, driving an electrical generator, providing ventilation, and agitating water to keep stock ponds ice-free during the winter [9,10]. Savonius rotor has a high starting torque and a reasonable peak power output per given rotor size, weight and cost, thereby making it less efficient [11]; the coefficient of performance is of the order of 15% [12,13].

The above advantages may not outweigh its low efficiency and make it an ideal economical source to meet small-scale power requirement. The concept of the Savonius

rotor was based on the principle developed by Flettner. Savonius used a rotor that was formed by cutting the Flettner cylinder into two halves along the central plane and then moving the two semi cylindrical surfaces sideways along the cutting plane so that the cross-section resembled the letter "S." A Savonius design was selected because of its greater simplicity in design and manufacture [14]. Savonius turbine relies on stagnation principles to convert current into rotational energy.

3. Numerical Analysis Method

Computational Fluid Dynamics is an important tool to recreate phenomena such as ocean wave and thus aids in understanding the hydrodynamics of it. As the increasing use of CFD in engineering analysis is evident it is important to make sure that the results from the simulation are in tandem with the theoretical or published results. For the numerical analysis of the savonius turbine, a commercial code ANSYS-CFX(11) is adopted. The numerical wave tank (NWT) is the basic building block to which various features that warrant consideration (e.g. an OWC) may be added. It is thus of fundamental importance that the NWT provide results with an appropriate degree of accuracy to ensure that results from subsequent modeling are not distorted or diminished.

Modeling of geometry was done in Unigraphics 4 and meshing was done using ICEM CFD AI Environment. Dimensions of the computational domain are given in Figure 2.

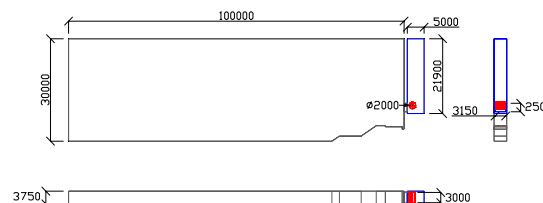


Fig. 2 Schematic diagram of the numerical wave tank

The two rotor configurations which was incorporated the simulations are shown below.

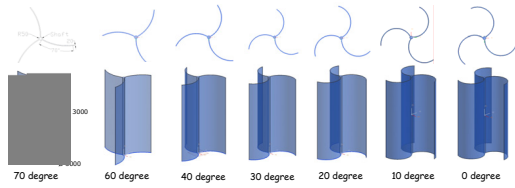
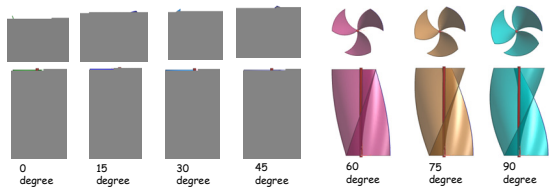


Fig. 3 Geometric view of 3 blade savonius rotor with various rotor angle.

Fig. 3 Geometric view of various 3 blade helical savonius rotor.



Structured grids were generated for all the cases using blocking arrangements. The total approximate accumulative grid number of 8×10^5 has been used for both the models as shown below. Fine hexahedral-grids are employed to ensure relatively high accuracy of calculated results for the turbine model. Finer mesh was adopted near the free surface level, to capture more accurate movement of free surface shown in Figure below.

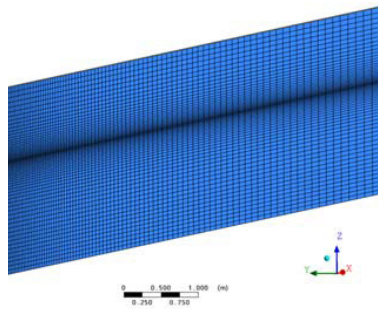


Fig. 3 Typical mesh for 2D wave maker (Refined mesh near the free surface)

4. Boundary conditions

A numerical wave tank has been modeled whose dimension was taken as an experimental wave tank. Waves are generated using a piston wave-maker. The solution domain is bounded by a wave maker on the left wall boundary. At the wave maker boundary, the horizontal velocity of motion of the boundary is imposed on the water particle velocities at the boundary. The other boundaries of the solution domain

are solid walls where no-slip boundary conditions are applied. The no-slip condition ensures that the fluid moving over a solid surface does not have velocity relative to the surface at the point of contact. Motion of the flap was implement through mesh motion giving specified displacement using CFX Expression Language (CEL). See Equation 1.

$$Y_{dis} = a \sin wt \quad (1)$$

A homogeneous model was adopted with k-Epsilon turbulence model for two phase calculations. Global initial condition was set to velocity in all the direction as zero, static pressure as hydrostatic pressure with turbulent KE and eddy dissipation rate as automatic with value.

5. Results and Discussion

5.1 Wave Simulation

Physical parameters of a wave in wave tank mainly depend on three factors namely water height, piston displacement and period of stroke displacement. At constant piston stroke length and at constant water height, dependency of the wave height elevation with same period was simulated and used for all the cases.

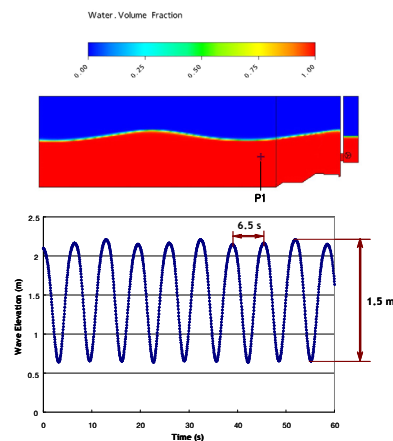


Fig. 5 shows the time history of wave elevation predicted at P1 (Fig.1) in the tank for turbulence model as K-ε turbulence model.

Table 1 Wave conditions and analysis

Period (s)	6.5
Wave height (m)	1.5
Water Level(m)	16.15
Turbine RPM	20
Average Torque (kN.m)	2.77
P _{Tave} (kW)	4.93
P _{wave} (kW)	43.39
WaveEnergyFlux(kW/m)	11.36

3.2 Turbine Performance Analysis

The optimization of the turbine depends on whether the turbine rotational speed N can be controlled to match the individual sea states, or is kept constant all the time. Obviously the first alternative is expected allow a higher energy production. The main advantage of constant rotational speed is to allow cheaper electrical equipment to be employed. However, power electronics and variable rotational speed generators are now relatively inexpensive and have been adopted in most, or all, recent OWC prototypes. An additional advantage of variable rotational speed is to allow energy to be stored as kinetic energy in, and released from, the rotating parts (flywheel effect), thus producing a smoothing effect on the electrical energy delivered to the grid; this is especially important in small grids. Here, even when variable rotational speed is being simulated, N is assumed to remain unchanged over each individual sea state. This is obviously not a very suitable control strategy, unless a very large set of sea states is considered. If this is the case, and if the inertia of the rotating parts is large enough, then it is reasonable to assume that the oscillations in N are relatively small over the duration of each individual sea state (say a few wave periods), and that N varies smoothly over longer time scales. For practical reasons of numerical simulation and since the rotational speed control is not the primary objective of the present paper, the optimum Savonius turbine rotational speed is found to be 20RPM through the Morrison's Equation.

5.2 TOTAL EFFICIENCY

Efficiency of a Savonius Type Turbine wave energy converter can be calculated by the following equation (Orer et al., 2007).

$$\eta = \frac{P_{Tave}}{P_{Wave}} \quad (2)$$

where P_{wave} and P_{Tave} are wave power and average torque power generated by the Savonius type turbine, respectively. P_{wave} and P_{Tave} are given by the following equation:

$$P_{wave} = \frac{1}{16} \rho g H_i^2 \frac{\lambda}{T} b \left[1 + \frac{\frac{4\pi d}{\lambda}}{\sinh \frac{4\pi d}{\lambda}} \right] \quad (3)$$

$$\begin{aligned} P_{Tave} &= \tau \omega \\ &= \tau \left[\frac{2\pi N}{60} \right] \end{aligned} \quad (4)$$

where d is the water depth, b is width of the chamber opening, λ the wave length, H_i the incoming wave height, ρ the water density (998kg/m³), g the gravitational acceleration (9.81m/s²), T the wave time period, τ the average torque, N the RPM of the turbine.

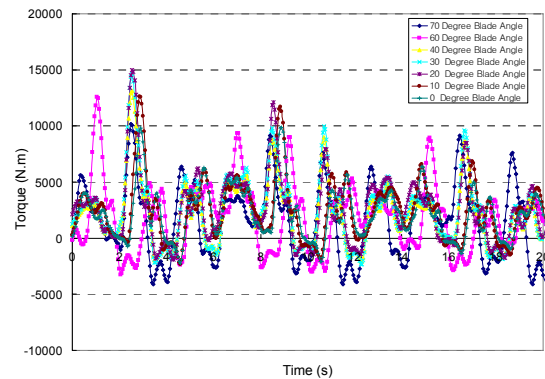


Fig.6 Instantaneous Torque of the various savonius rotor angles with numerical time integration scheme

Table 2 Performance analysis of various savonius rotor blade angles

Balde angle, ⁰	Torque, kN.m	P _{ave} , kN.m	Efficiency, %
70	2.4	5.03	11.58
60	2.73	5.72	13.18
40	3.25	6.81	15.69
30	3.62	7.58	17.47
20	3.85	8.06	18.58
10	3.59	7.52	17.33
0	3.29	6.89	15.88

Simulation results show smooth running, higher efficiency and self starting torque capability of the 20⁰ rotor compared to that of the other rotor.

It can also be seen from the table that the difference in average torque between the highest and the lowest is 1.45 kN.m. Thus, at given wave conditions, rotor angle of 20⁰ is preferable for its highest efficiency of 18.58%.

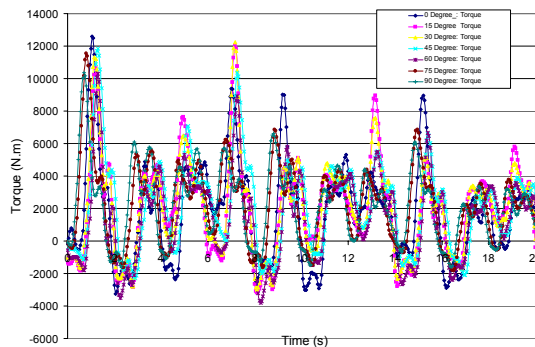


Fig.6 Instantaneous Torque of the various helical savonius rotor with numerical time integration scheme

Table 2 Performance analysis of various savonius rotor blade angles

Helical blade angle, ⁰	Torque, kN.m	Pave, kN.m	Efficiency, %
Base model	2.73	5.72	13.18
15	2.96	6.20	14.29
30	3.04	6.37	14.67
45	3.2	6.70	15.45
60	3.27	6.85	15.78
75	3.34	7.0	16.12
90	3.3	6.91	15.93

The maximum efficiency of 16.12% was obtained at 75⁰ helical twist.

5.3 Flow Characteristic in and around Savonius Rotor

The rotor is well aligned to receive the energy of the wave and the direction of rotation is matching the wave force. The direction of rotation of the rotor is always anti clock-wise when the wave motion is in x-direction. The velocity vectors at a frequency of 0.15 Hz, wave height of 1.5m and period of 6.5s for the case when the water velocity is the maximum is shown in the figures respectively.

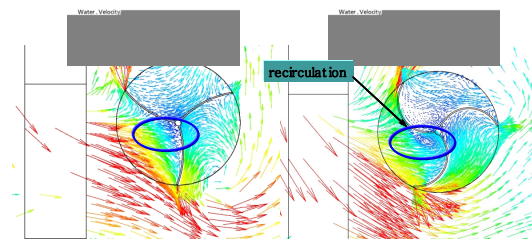


Fig. 7 Velocity vector at maximum torque

The Figures above shows respectively, the phase vector velocity distributions in and around the rotating savonius rotor at two rotor blade angles 70⁰ and 20⁰. A dramatic change in the field is observed in the 20⁰ figure in comparison to 70⁰. It is observed that the internal velocity on the advancing side is accelerated and that on the returning side, by the presence of circulation produced by the curved rotating rotor, which is not observed for the 70⁰ rotor.

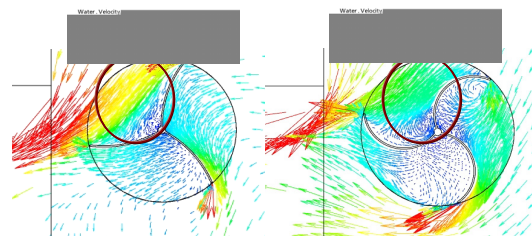


Fig. 8 Velocity vector at manimum torque

The flow in side the rotor moves form the advancing side of the blade to the returning

side of the rotor, thus producing a torque recovery effect on the concave side of the returning blade. This phenomenon is closely related to the appearance of favorable pressure on the concave side of the rotor as seen in the torque graph which contributes largely to the production of anticlockwise rotating torque.

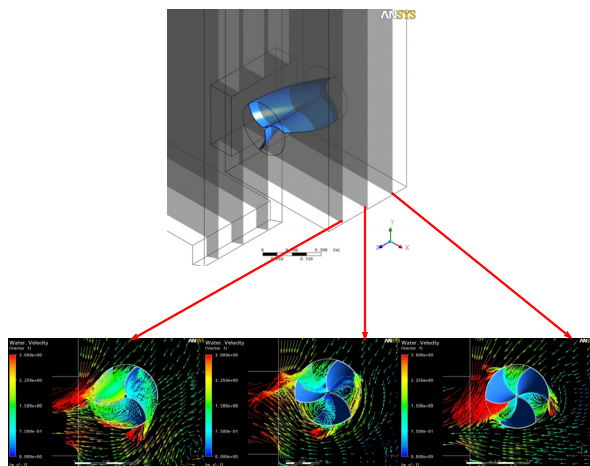


Fig. 9 Velocity vector at the 3 planes at the same instantaneous time.

In the conventional blade, the maximum force acts centrally (curvature center) and vertically, whereas for the helical blade, the maximum force moves towards to the tip of the blade because of the twist in the blade as can be seen in the plane velocity figure above. Due to these changes, a twisted blade gets a longer moment arm, and hence a higher value of net positive average torque.

6 Conclusion

In summary, CFD simulation studies show the potential of the savonius rotor for wave energy conversion. The aerodynamic characteristic of the rotating savonius rotor is much improved by the 20° savonius rotor blade and also by the 75° helical blade.4%. The simulated wave energy flux is 13.77kW/m. The highest total efficiency is 18.58% for the 20° savonius rotor angle and 16.12% for the 75° helical savonius, therefore the rotor converts 2.48kW/m and 2.22 kW/m respectively. Three-bladed conventional savonius rotor is well known for its self-starting

characteristics and it has been improved by a higher savonius rotor angle and also by a helical twist.

References

- [1] "Waves and Swell," NOAA Library's Oceanic and Atmospheric Sciences, .
- [2] Boud, R., 2003, "Status and Research and Development Priorities, Wave and Marine Current Energy," UK Dept. of Trade and Industry (DTI), DTI Report # FES-R-132, AEAT Report # AEAT/ENV/1054, United Kingdom.
- [3] Falnes, J., 2007, "A review of wave-energy extraction," *Marine Structures*, Vol. 20, pp. 185-201.
- [4] Holthuijsen, L.H., 2007, *Waves in oceanic and coastal waters*, Cambridge Univ. Press, United Kingdom.
- [5] Mehaute, B.L., 1976, *An introduction to hydrodynamics and water waves*. 1st ed., Springer, New York.
- [6] Twidell, J., Weir, A.D., 2006, *Renewable energy resources*, 2nd ed., Taylor and Francis, New York.
- [7] Pelc, R., Fujita, R.M., 2002, "Renewable energy from the ocean," *Marine Policy*, Vol. 26, pp. 471-479.
- [8] McCormick, M.E., 2007, *Ocean wave energy conversion*. 1st ed., Dover Publications, New York.
- [9] Modi, V.J., Roth, N.J., Pittalwala, A., 1981, "Blade configuration of the Savonius rotor with application to irrigation system in Indonesia," In: *Proceedings of 16th inter society energy conversion engineering conference*, Atlanta, GA, USA.
- [10] Vishwakarma, R., 1999, "Savonius rotor wind turbine for water pumping—an alternate energy source for rural sites," *Journal of Institution of Engineers (India)*, Vol. 79, pp. 32-34.
- [11] Reupke, P., Probert, S.D., 1991, "Slatted-blade Savonius wind-rotors," *Applied Energy*, Vol. 40, pp. 65-75.
- [12] Kumar, A., Grover, S., 1993, "Performance characteristics of a Savonius rotor for wind power generation—a case study, alternate sources of energy," In: *Proceedings of ninth national convention of mechanical engineers*. India: IIT Kanpur.